EVS30 Symposium
Stuttgart, Germany, October 9 - 11, 2017

Model Identification for Thermal Modelling of a Battery Pack

Steven Wilkins[1,3], Stefan van Sterkenburg[2], Erik Hoedemaekers[1],
Bogdan Rosca[1], Dmitry Danilov[3], Rik Baert[1,4]

[1]*TNO, Dept. of Powertrains, Helmond, Netherlands (corresponding author: steven.wilkins@tno.nl)*

[2] *HAN University of Applied Sciences, Ruitenberglaan 29, 6826CC Arnhem, the Netherlands*

[3]*Dept. of Electrical Engineering, Eindhoven University of Technology, Netherlands*

[4]*Fontys Automotive Center of Expertise, Helmond, Netherlands*

Executive Summary

Thermal pack management is dependent on the duty cycle and vehicle use. Thermal modelling of the pack for design, as well as active measures in operation to reduce thermal loads during operation can greatly improve the lifetime of the pack. Advances in state estimation, measurement techniques and control are coupled with the system design; and both are dependent on representative models. As the cells age, the thermal behaviour will change, and therefore a robust control technique and in-situ thermal model identification is often required. This paper focuses on methodologies towards thermal characterization of cell models and of a pack as a whole.

Introduction

Advances in battery technology, combined with the need for higher power levels of fast charging place increasing demands on both understanding and modelling of automotive battery packs. During the design process, as well as during operation, it is important to maintain accurate models for both individual cells, as well as complete modules/packs.

In general a battery model for systems analysis commonly consists of electric and thermal sub-models. The electric sub-models also characterize the heat dissipation inside each cell. It is possible choose to use equivalent network models of the battery cells, such as to reflect both the electrical and thermal properties.

An equivalent network model of a battery cell generally consists of a voltage source (the open circuit voltage) and an impedance that exists of a single resistor in series with multiple RC-networks. The values of most network components depend on temperature and State of Charge (SoC), and as such an integrated approach to both thermal and electrical modelling is required. Due to this integration, and the accumulation of errors between the modelling domains, thermal modelling at a pack level remains a challenging field of research.

The thermal sub-models model the temperature of each cell, and the interactions of the cell thermally with its surroundings (including other cells). It can be assumed that the temperature within a cell may be considered to be uniform, in order to simplify the modelling task. Due to this assumption, it is possible to model each cell as a combination of a heat source, heat capacitance, and heat resistors that connect one cell to adjacent cells and ambient. The power of the heat sources can be set to equal the electric current multiplied by the overvoltage of each cell and is modelled by the electric sub-model.

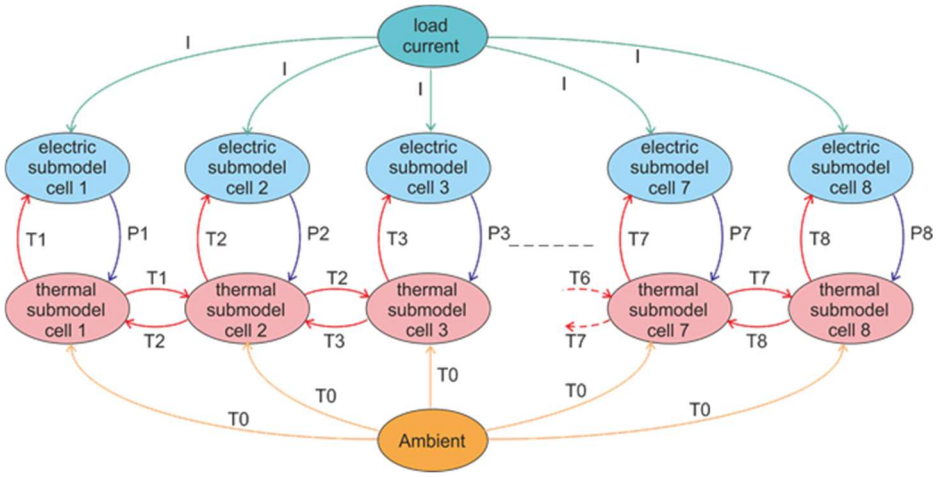

Figure 2. Data flow diagram of the battery model presented in this paperp

The load current and ambient conditions are the global inputs of such a model. The cell temperatures are the global output of the model, commonly used for systems analysis. Figure 2 shows a data flow diagram of the complete battery model, and Figure 3 illustrates a schematic of a coupled electrical-thermal battery model.

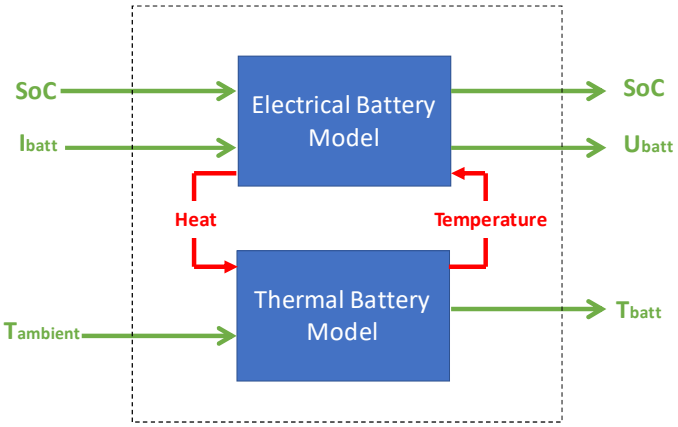

Figure 3. Functional schematic for a coupled electrical-thermal battery model

Due to the inter-dependency of the electrical and thermal models, there is often a challenging task in providing representative models to predict temperatures. Moreover, as the cells age, their parameters (particularly impedance) vary, making temperature predictions less accurate whilst using parameters obtained only from new cells. Small errors in models can lead to accumulated inaccuracies over long periods in predicting future temperatures.

Electric Model of Battery Cell

Electric model characterization tools for cell-level have been well published in literature. In this paper two different electric cell models are considered. One model is obtained from the AMESim battery assistant, a commercially available tool. This tool models the electrical behaviour of a cell by a 5th order equivalent network model (see Figure 4). The behaviour of the network components of the AMESim model is stated to depend on the SoC and temperature.

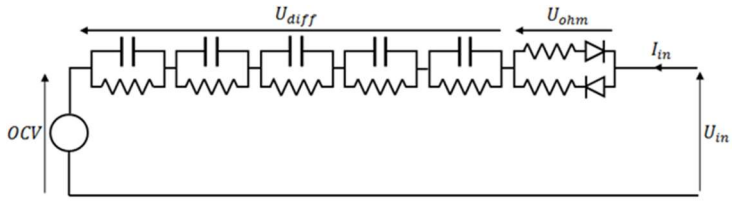

Figure 4. The equivalent network model that is used by the AMESim battery assistant tool

The tool determines the model parameters from identification measurements carried out at different temperatures. Such an identification measurement is a measurement of cell voltage when the battery is loaded by a current profile that exists of multiple charge/discharge current pulses with different pulse lengths carried out at different state of charge levels [1]. Figure 5 shows the current profile that have been used for the AMESim battery assistant tool. One complete identification measurement at one temperature lasts about nine hours. Measurements were carried out at 0°C, 10,°C, 20°C, 30°C and 40°C.

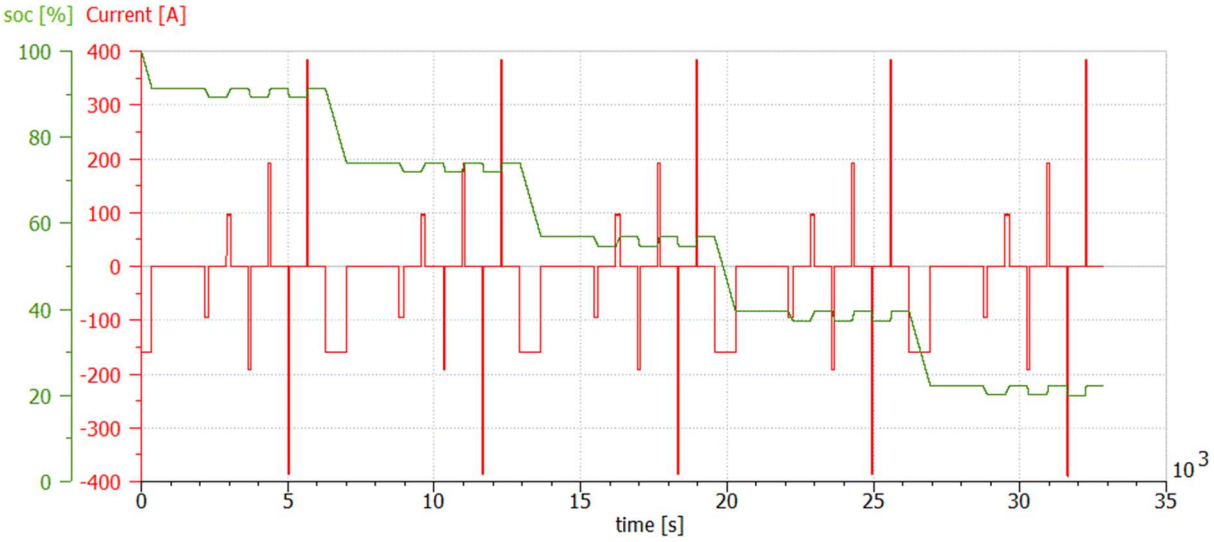

Figure 5. Current profile that is used for the AMESim battery assistant tool

Within this paper the electric cell model obtained from the AMESim battery assistant tool is compared to a commonly applied second order cell model [2] (see Figure 6). As part of this investigation, a Thundersky 160Ah battery cell was targeted, with a small pack of eight of these cells arranged in series.

The result of the AMESim battery assistant tool is a battery cell model that includes a set of lookup-tables which give the model parameters of Figure 4 as a function of temperature and state of charge. Electrical parameter identification takes place using a pulsed charge profile such as that illustrated in Figure 5.

For the second order model, an identification process was required. This process is described as follows. The open circuit voltage (OCV) of this second order model was obtained by a

discharge/charge current measurement at a relatively low C-rate of 0.1C. Later, a compensation for the internal voltage losses across the impedance was applied.

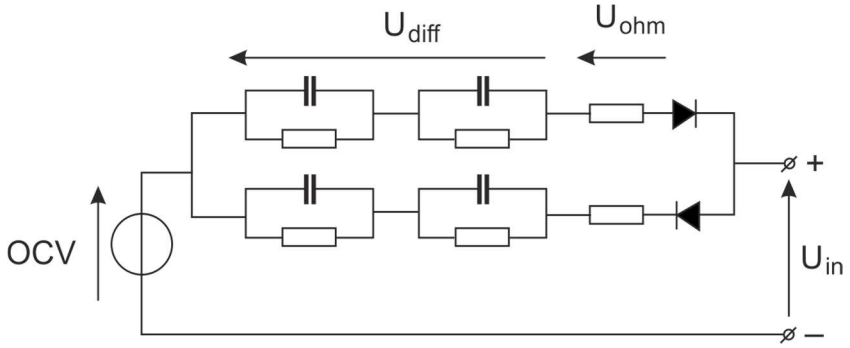

Figure 6. Second order cell model, similar to those commonly found in literature

The internal impedance is determined by a white noise pulse current measurement at different state of charge levels. The white-noise pulse period starts with a rest period of 2550 [s] followed by a series of 255 current pulses, each having a pulse width of 10 [s] and a random current strength with a white noise spectrum. Figure 7 shows the current shapes of the OCV and impedance measurements. The measurements were carried out at temperatures of 0°C, 20°C and 40°C.

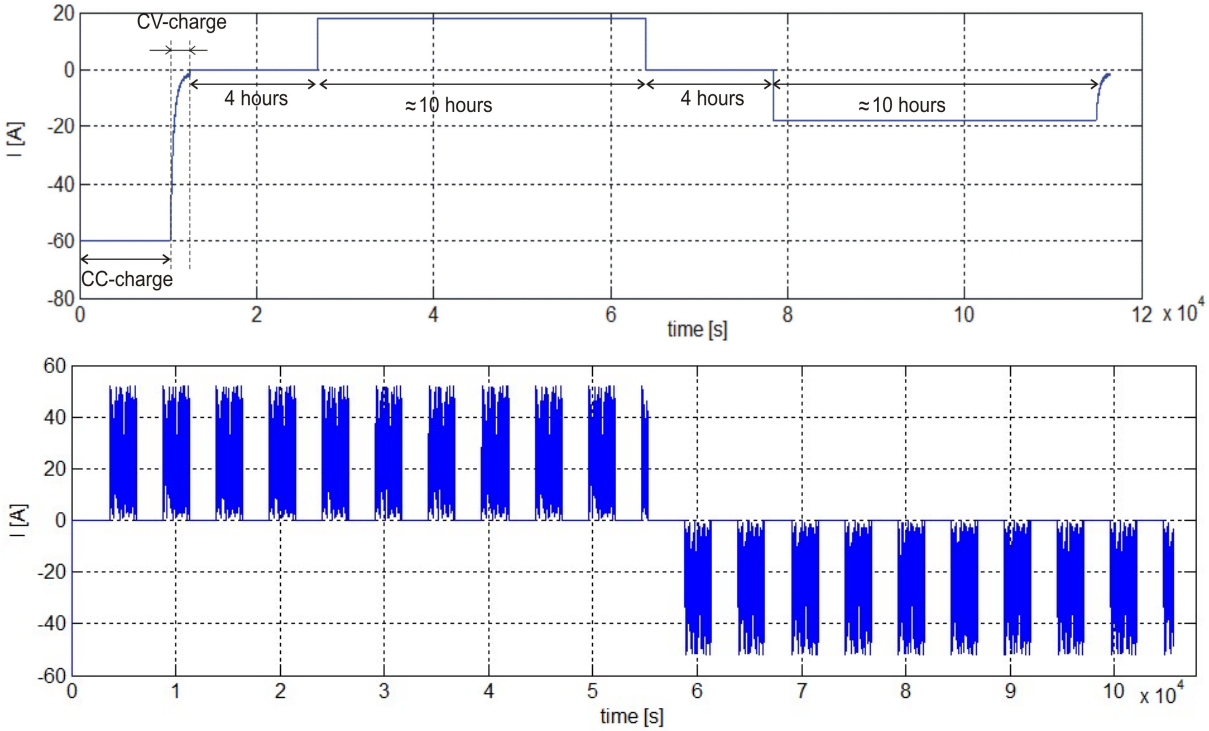

Figure 7. The upper graph shows the current that is used to determine the OCV as a function of the SoC. The lower graph shows the current profile used to determine the impedance.

The Matlab system identification tool ('tfest.m') was used in order to determine the model parameters. All model parameters are also functions of state of charge and temperature, given the strong interdependency of these factors.

Validation Of Electric Cell Models

The electric cell models were both validated in two ways, described below.

Firstly, the modelling of the terminal voltage was validated, using an application-specific duty cycle. For this, a current profile that was recorded from an electric *Fiat Doblo* that drove the NEDC. The cell repeatedly loaded with this current profile, until the cell voltage dropped below the 2.4V. In between two current profiles, a rest period of five minutes was included.

The measurements were carried out at 0°C, 20°C and 40°C. Due to cell limitations, it was possible to load the cell with seven complete NEDC currents profiles at a temperature of 20°C and 40°C and 5 complete cycles at 0°C. Figure 8 shows the current profile and some of its characteristics.

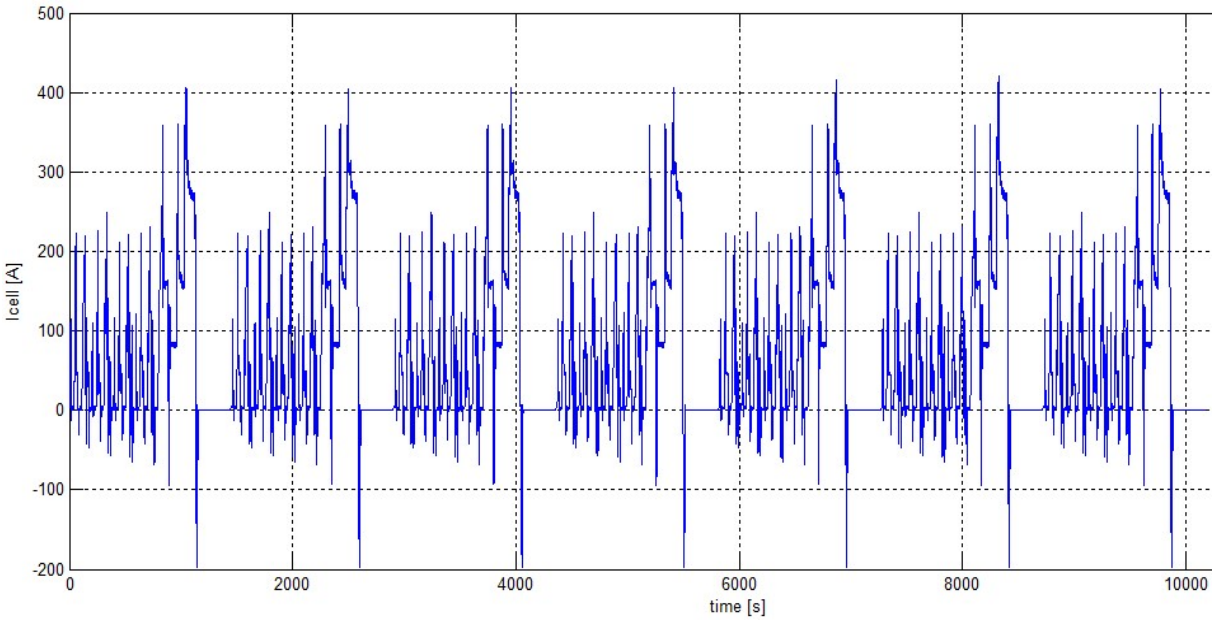

Figure 8. The validation current consists of multiple current profiles with a rest period of 300 s in between them. The following applies per NEDC current profile: $I_{average}$ = 62.9 [A], I_{eff} = 114.6 [A] and DDOD = 25.4 [Ah]

Figure 9 shows the graphs of the measured and modelled voltages.

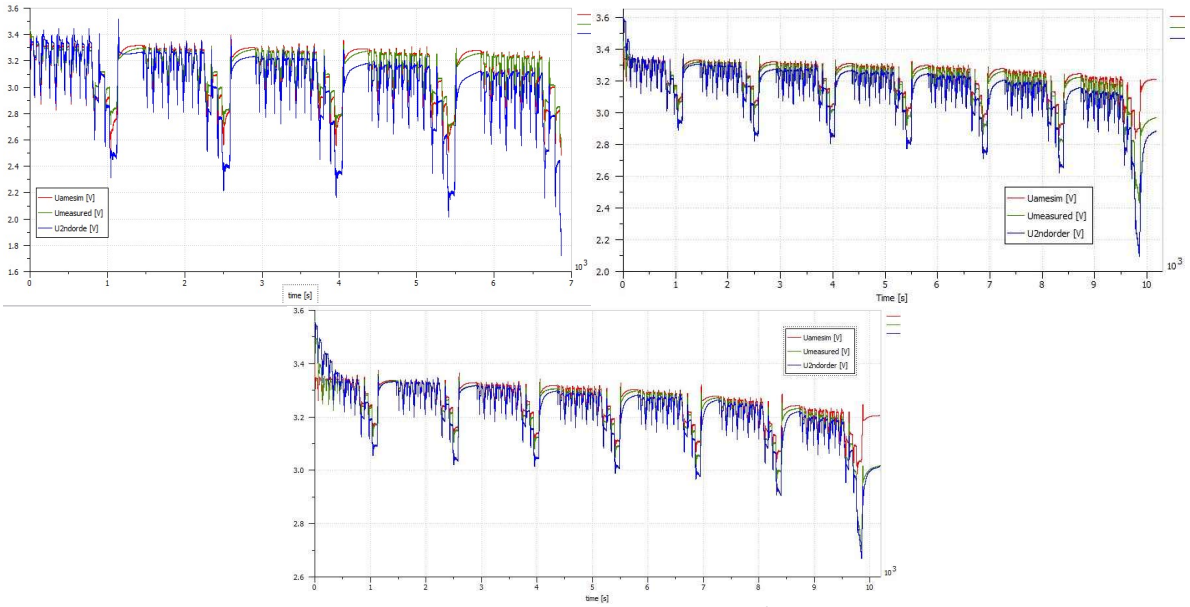

Figure 9. The validation voltage error comparing the AMESim and 2nd Order Model across the test cycle, taken at 0°C (top left), 20°C (top right), and 40°C (bottom)

Table 1 shows the effective error of the AMESim model and 2nd order model as a function of the temperature. The effective error is defined as:

$$effective\ er \qquad \sqrt{\frac{\int_0^T (U_{measurement} - U_{model})^2\, dt}{T}} \qquad where: T = tim \quad span\ of\ measurement$$

Table 1. Effective error in [mV] between the measured and modelled voltage of the validation measurement

Temperature [°C]	Effective error AMESim model [mV]	Effective error 2nd order model [mV]
0	42	177
20	67	77
40	50	30

The second series of validation measurements relate to the calculation of the power losses. In order to measure the power losses, the cell were loaded with symmetrical discharge/charge pulses with a pulse length that varied from 1 [s] to 512 [s]. The discharge current was 90A and charge current was -90A for the discharge/charge pulses of which the pulse length is smaller than 256 [s]. The discharge current was 60A and charge current was -60A for pulses with a pulse length of 256[s] and 512 [s]. Each series of discharge/charge pulses is followed by a 10% discharge current and a zero current rest period of 1 hour. In this way, the power losses were determined at SoC-levels form 95% to 15%. Figure 10 shows the validation current.

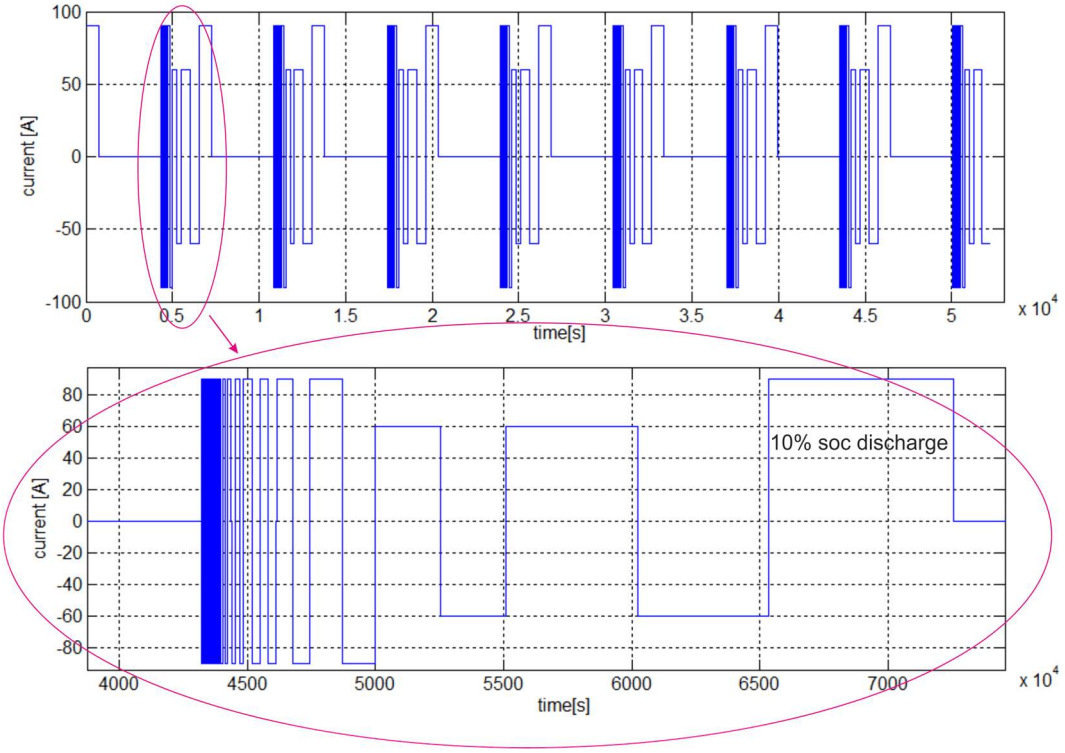

Figure 10: Current of the power validation measurements. The pulses with a pulse length shorter than about 8 [s] are not visible due to the resolution of the graph.

Due to each discharge/charge pulse being symmetrical, there is no net electrochemical conversion of energy. As such, all energy input of the battery is converted to heat and can be calculated from the measured or simulated voltage and current as:

$$W_{cycle} = \int_0^{T_{cycle}} U_{cell} \cdot I \cdot dt \quad \rightarrow \quad P_{cycle\_average} = \frac{W_{cycle}}{T_{cycle}} = \frac{\int_0^{T_{cycle}} U_{cell} \cdot I \cdot dt}{T_{cycle}} = \left(U_{charge\_average} - U_{discharg\ \_average}\right) \cdot I_{abs}$$

Where:

- I_{abs}= the (absolute) value of the current during the charge/discharge cycle
- $P_{charge\_average}$ = the average power dissipation during one discharge/charge cycle
- $U_{charge\_average}$ = the average cell voltage during charging
- $U_{discharge\_average}$ = the average cell voltage during discharging
- T_{cycle} = time span of one discharge/charge cycle.

Table 2. Average error in [%] between the modelled power dissipation.

Temperature [°C]	average error AMESim model [%]	average error 2nd order model [%]
0	7.2	12.3
20	13.6	10.1
40	6.6	6.4

Thermal Model Of Battery Pack in AMESim

The electric sub-models of the eight cells are identical and are obtained from the AMESim battery assistant tool. The heat generation inside a cell is modelled by AMESim by calculating the product of the overvoltage of and the electric current. A thermal model was set up based on the following assumptions:

- Each cell is modelled as one heat capacity that has a uniform temperature. Literature shows that temperature variations within a cell are in general less than 10% compared to the temperature rise of a cell ([3], [4]).
- Adjacent cells exchange heat mutually by means of heat conduction
- Cells exchange heat to the exterior of the battery pack through heat conduction.
- The battery pack exchanges heat to the environment by conduction. The heat capacitance of the battery pack case is neglected.
- Heat conduction takes place through the current cables on the corner cells. The heat dissipation and heat capacity of the current cables is neglected.

Figure 11 show the heat flows from cell to cell and from cell to environment.

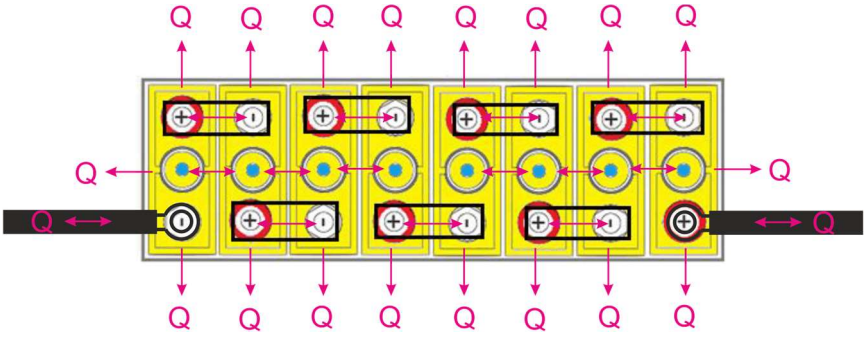

Figure 11: Top view of the battery pack. The pink arrows indicate the heat flows from cell to cell, inside the pack, and from cell to environment

Figure 12 shows the AMESim battery pack model.

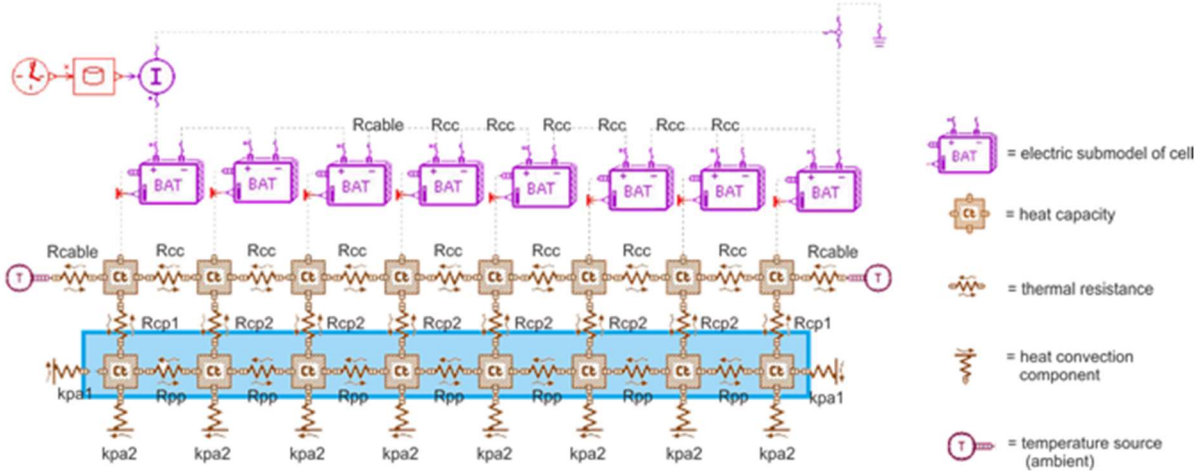

Figure 12: Thermal RC-model of the battery pack

The thermal model of Figure 12 holds the following parameters:

- C_{cell} = Heat capacitance of one cell (the upper row of heat capacities in Figure 12)
- C_{pack1} = Heat capacitance of the section of the battery pack that surrounds a corner cell (the most left and most right heat capacitance on the lower row of heat capacities in Figure 12).
- C_{pack2} = Heat capacitance of sections of the battery pack that surround non-corner cells (all other heat capacities on the lower row of heat capacities in Figure 12).
- R_{cable} = Thermal resistance from corner cell to environment via the current cable.
- R_{cc} = Thermal resistance between two adjacent cells
- R_{cp1} = Thermal resistance between corner cells to exterior of battery pack.
- R_{cp2} = Thermal resistance between non-corner cells to exterior of battery pack.
- R_{pp} = Thermal resistance between adjacent sections of the battery pack
- k_{pa1} = Thermal convection from exterior of corner cell section of battery pack to ambient
- k_{pa2} = Thermal convection from exterior of non-corner cell section of battery pack to ambient

Thermal Model Parameters Estimation

The heat capacity of a cell was estimated by determining the heat exchange of a cold cell placed in a thermally isolated box with warm water. The thermal capacity of the cell is calculated from the energy balance as:

$$C_{cell} = \frac{C_{water} \cdot \left(T_{water}(t_0) - T_{water}(t_1)\right) - \int_{t0}^{t1} P_{box \rightarrow environment} \cdot dt}{T_{cell}(t_1) - T_{cell}(t_0)}$$

Where: C_{cell} = heat capacity of a cell

- t_0 = time at beginning of measurement
- t_1 = time at end of measurement
- T_{water} = water temperature
- C_{water} = heat capacity of the water (16.3 kJ/K).
- $P_{box \rightarrow environment}$ = heat loss of box to the environment

From this measurement, a value of the heat capacity was found of: C_{cell} = 4.8 [kJ/K]. The specific heat capacity of this cell is: 4.8 [kJ/K] / 5.53 [kg] = 0.87 [kg/(J·kg)] which is in fair agreement with values found in literature [5].

Heat Capacity Battery Pack Sections

The heat capacity of each section of the battery was determined by estimating the volume of each section and multiplying this with the specific mass and specific heat of the battery pack material (polypropylene, r_m = 900 [kg/m^3], $C_w = 1.9 \cdot 10^3$ [J kg^{-1} K^{-1}] [6]).

In this way we found for the heat capacities of the pack sections at the corner cells:

- Volume non corner cells = $3.9 \cdot 10^{-4}$ m^3 $C_{pack1} = 6.7 \cdot 10^2$ [J/K]
- Volume corner cells = $7.1 \cdot 10^{-4}$ m^3 $C_{pack2} = 1.2 \cdot 10^3$ [J/K]

Thermal Resistance Cable To Environment

The thermal behaviour of the cable depends on several factors such as the length of the cable and to the way the other end of the cable is connected (for instance, it might be connected to a heat sink of a supply or to a fuse).

In the test case, the cable length is much longer than the factor g defined as: $g = (A \times k_{cu}) / k_{ca})^{0.5}$ with:

- A = cross section of cable in [m^2]
- k_{cu} = thermal conductivity of cupper or other metal of which the cable is made in [W/(K·m)]
- k_{ca} = heat conductance of cable to environment of cable in [W/(K·m)]

In that case, the heat resistance R_{cable} in the model of Figure 12 can be approximated by:

- $R_{cable} = (A \cdot k_{cu} \cdot k_{ca})^{-0.5} = 9.9$ [K/W]

Thermal Resistance Between Adjacent Cells

The thermal resistance between two adjacent cells was determined by measuring the temperature of a warm cell that that is placed next to a cold cell in a thermally isolated box. The copper connection strip between the two cells was connected because it is expected to have a significant contribution to the overall thermal resistance between two cells. A value of: R_{cc}=2.1 [K/W] was determined.

Thermal Resistance Between Battery Pack Sections

The thermal heat resistance was determined between adjacent sections of the battery pack from the thermal conductivity of polypropylene and the dimensions of the sections. For the thermal conductivity, a value of 0.15 [W m^{-1} K^{-1}]) was used. A value of R_{pp} = 0.075m / (0.0052m^2 · 0.15) = 96 [K/W] was used.

Thermal Resistance Between Cells And Exterior Of Battery Pack

The thermal resistance between cells and exterior of battery pack consists of several parts, such as the thermal conduction through the cell case and pack case and the contact resistance between cell and pack.

The total thermal resistance was measured by heating the complete battery pack in a temperature chamber to about 45°C. Then, the pack was allowed to cool down in the ambient temperature of the laboratory. While cooling down, the ambient temperature was measured, and the temperature of six cells and the temperature on the exterior of the battery pack at six different locations was also monitored. From this measurement the thermal conductivity k_{cp} was calculated between cells and exterior of battery pack by:

$$k_{cp} = W_{heat} / (\int(DTdt) * A)$$

where:

- W_{heat} = energy loss of the cells in time interval $t_0 \leq t$ £ t_1.
- DT = average temperature difference between cells and exterior of battery pack
- A = surface area of exterior of battery pack

The selected limits of the time-interval in which we determined the conductance at t_0 = 600 [s] and t_1= 3000 [s]. The energy loss of the cells is calculated according to:

$$W_{hea} = C_{cell} \cdot \sum_{i=1}^{8} T_{cell}(t_0) - T_{cell}(t_1)$$

Since it was not possible to measure all cell temperatures in one measurement, the cell temperatures of the cells was determined by a weighted average based on the measured temperatures by nearby sensor signals and the symmetry of the pack.

The average temperature between cells and exterior of battery pack is determined by a weighted average of the temperature difference between two opposite sensors. The weight factor used in the calculation depends on the symmetry of the pack and surface area that is covered by two opposite sensors.

Verification Methodology

In order to verify the functionality of the model, a symmetric loading profile (‘balanced use-case current profile) was used. For the series of verification measurements, the current profile shown in Figure 16. This current exists of a series of symmetrical charge/discharge pulses with an amplitude of 200[A] and -200[A] and a pulse length of 120 [s] and a one hour rest period. Also this validation measurement will be carried out at 0°C, 20°C and 40°C.

The same validation current was applied to the AMESim model and compared the measured and modelled temperatures at the poles of the cell and battery pack case, presented in the next section.

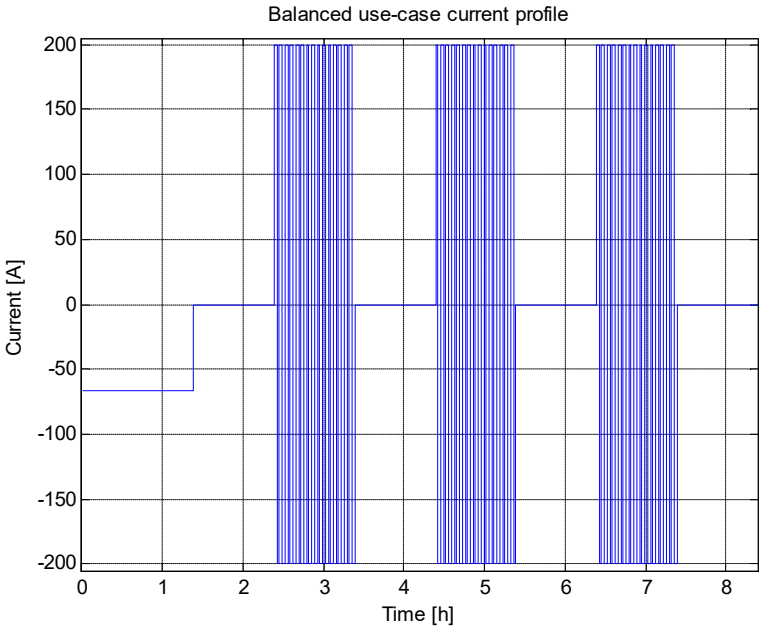

Figure 13 Balanced current profile used for verification measurements

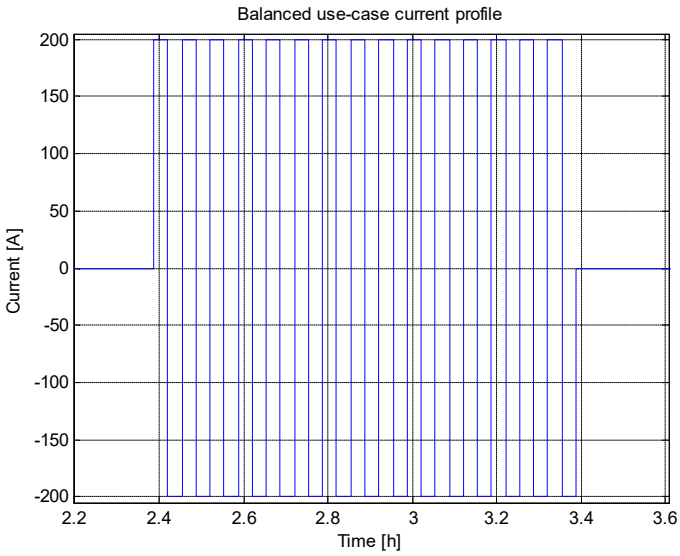

Figure 14: Balanced current profile - zoomed

Verification Measurements

The balanced current profile was compared with the fitted AMESim simulation results. Figure xx illustrates the testing results.

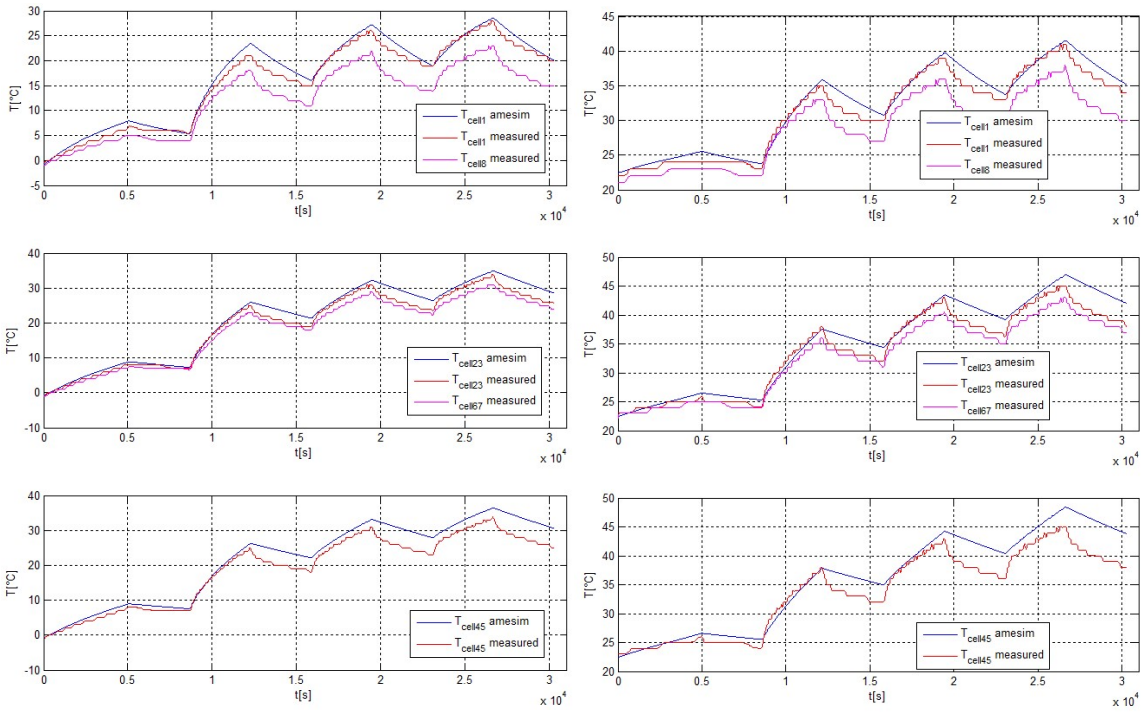

Figure 15: Temperature during balanced loading cycle, ambient of 0°C (left) and 20°C (right) (40°C is not shown)

In order to quantify the accuracy of the model, the effective temperature error is defined as:

$$\text{effective temperature error [\%]} = 100\% \cdot \frac{\sqrt{\frac{\int_0^{tend}(T_{simulation} - T_{measurement})^2 \cdot dt}{t_{end}}}}{\frac{\int_0^{T} \Delta T_{measurement} \cdot dt}{t_{end}}}$$

where:

- $T_{simulation}$ = simulated temperature, $T_{measurement}$ = measured temperature ,
- $\Delta T_{measurement} = T_{measurement} - \text{ambient}$ and t_{end} = end time of measurement

Table 3 Temperature errors for thermal pack model for new pack, for balanced current cycle

	T=0°C, ventilation on	T=20°C, ventilation on	T=40°C, ventilation on
cell1	9%	11%	14%
average of cell 2 and cell3	10%	14%	18%
average of cell 4 and cell5	16%	21%	23%
average of cell 6 and cell 7	17%	23%	28%
cell 8	38%	40%	38%
Average	**18%**	**22%**	**24%**

Table 4 Temperature errors for thermal pack model for aged pack, for balanced current cycle

	T=0°C, ventilation on	T=20°C, ventilation on	T=40°C, ventilation on
cell1	57%	85%	72%
average of cell 2 and cell3	44%	49%	61%
average of cell 4 and cell5	38%	50%	58%
average of cell 6 and cell 7	40%	49%	61%
cell 8	39%	50%	72%
Average	**44%**	**57%**	**65%**

Validation Methodology

In order to validate the model, the battery pack was subjected to an automotive test cycle generated from a simulation platform. For the case of brevity, this cycle is not described in detail, but is illustrated by Figure 16.

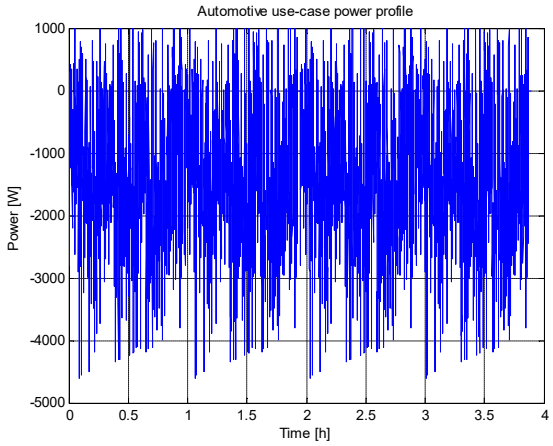

Figure 16: Automotive use-case power profile

The intent of the validation step is to assess the model accuracy against an intended application cycle, which was not used in the model identification process.

Validation Measurements

In a similar way to the verification method, the validation exposed the battery pack to automotive cycles. Figure 16 illustrates test results compared with the AMESim model.

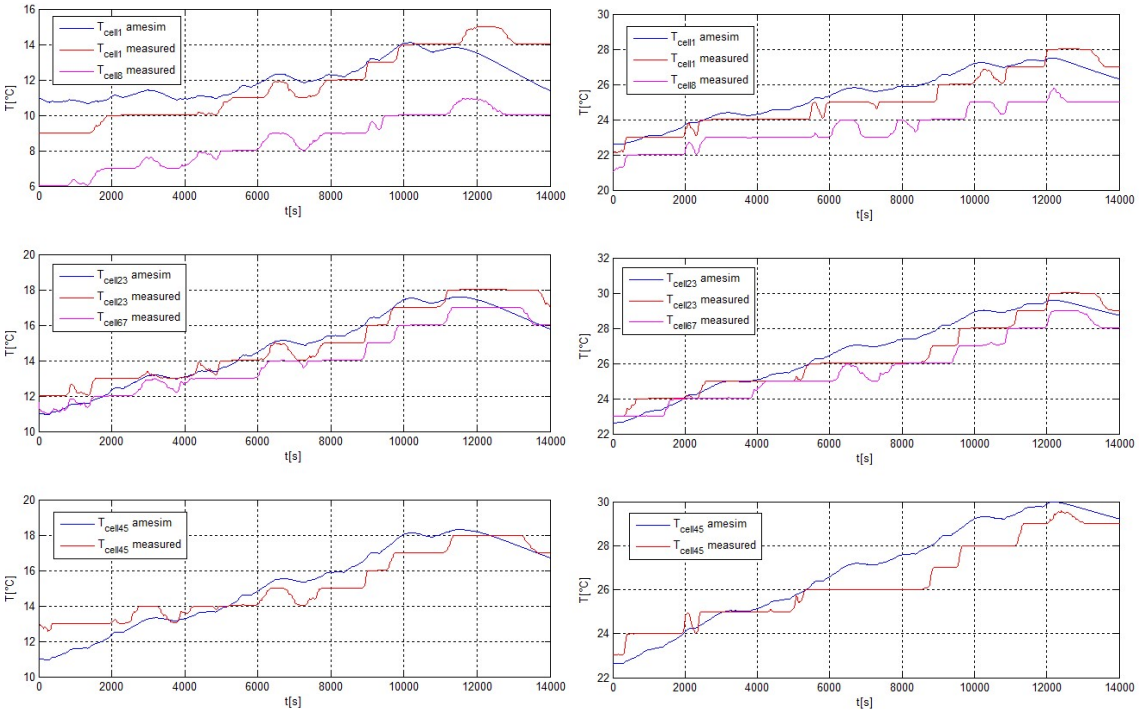

Figure 16: Automotive validation, , ambient of 0°C (left) and 20°C (right) (40°C is not shown)

Table 5 Temperature errors for thermal pack model for new pack, for automotive cycle

	T=0°C, ventilation on	T=20°C, ventilation on	T=40°C, ventilation on
cell1	10%	11%	17%
average of cell 2 and cell3	5%	11%	15%
average of cell 4 and cell5	6%	13%	16%
average of cell 6 and cell 7	7%	19%	21%
cell 8	43%	46%	45%
Average	**14%**	**20%**	**23%**

Table 6 Temperature errors for thermal pack model for aged pack, for automotive cycle

	T=0°C, ventilation on	T=20°C, ventilation on	T=40°C, ventilation on
cell1	62%	69%	66%
average of cell 2 and cell3	74%	80%	56%
average of cell 4 and cell5	44%	46%	54%
average of cell 6 and cell 7	43%	49%	56%
cell 8	51%	55%	66%
Average	**55%**	**60%**	**60%**

Conclusions

This work presented a thermal model of a battery pack that consists of interacting electric sub-models and thermal sub-models, made within a commercial tool, AMESim.

The electric sub-model is on a battery-cell level and calculates the heat dissipation in the cells. The AMESim-battery assistant tool to obtain an electric cell model, and was compared the accuracy of a second order cell model obtained from standard OCV and impedance measurements, and where the

parameter estimation has been carried out by using the Matlab system identification tool (tfest.m). The accuracy of the AMESim model was found to be better than the second order model at low temperature (0°C) and worse at higher temperatures (40°C). On average, the error in power dissipation modelling was determined to be ~10%.

The thermal sub-model consisted of heat capacities of cells that are connected to each other by thermal resistances and to the battery pack. Heat convection is assumed to be the dominant heat exchange from battery pack to ambient. Most thermal parameters were determined by relatively simple measurements. The challenge for this research area is that temperature prediction is based on the accumulation of small heat generations, and as a result errors can also accumulate in the simulation models [7, 8].

The overall model was verified by two tests on new and aged packs, with a specific loading test with measurements both at three temperatures (0°C, 20°C and 40°C). Model parameters were not updated for the aged pack so as to test the robustness of the model fit. The verification cycle accuracy of the new pack in terms of average temperature error was 18-24%, and 44-65% for the aged pack. For the automotive validation cycle, the errors on the new pack were 14-23%, and 55-60% for the aged pack. The differences in accuracies for the aged cells is likely to be on account of the increased impedances, compared with the fitted values to the new cells.

Acknowledgments

This work was funded by the RAAK-PRO QinE project funded by SiA. The authors kindly acknowledge also the involvement of other partners within this project.

References

[1] Julien Hafsaoui, Franck Sellier, "Electrochemical model and its parameters identification tool for the follow up of batteries ageing", World Electric Vehicle Journal Vol. 4 - ISSN 2032-6653 - © 2010 WEVA

[2] “Energy Storage Systems Solution.pdf”, a publication of LMS Imagine.Lab Amesim simulation solutions.

[3] Long Lam et. Al., A Practical Circuit-based Model for Li-ion Battery Cells in Electric Vehicle Applications, Telecommunications Energy Conference (INTELEC), 2011 IEEE, ISSN: 2158-5210

[4] Yong Liu, Shichun Yang, Bin Gu and Cheng Deng, “Numerical Analysis and Design of Thermal Management System for Lithium Ion Battery Pack Using Thermoelectric Coolers”, Hindawi Publishing Corporation Advances in Mechanical Engineering, Volume 2014

[5] S. C. Chen, C. C. Wan, and Y. Y. Wang, “Thermal analysis of lithium-ion batteries,” Journal of Power Sources, Vol. 140, no. 1, pp. 111–124, 2005

[6] Ahmad A. Pesaran and Matthew Keyser, “Therma/l Characteristics of Selected EV and HEV Batteries”, National Renewable Energy Laboratory, 2009

[7] Mojtaba Shadman Rad, Dmitri L. Danilov, Morteza Baghalha, Mohammad Kazemeini, Peter H. L. Notten, “, Thermal Modeling of Cylindrical LiFePO4 Batteries”, Journal of Modern Physics, 2013, 4, 1-7

[8] Bogdan Rosca, Steven Wilkins, Enhanced battery model including temperature effects, Electric Vehicle Symposium 27, Barcelona, 2013

Authors

Dr. Steven Wilkins works as a scientific research engineer with a background in hybrid and electric vehicle systems and powertrain modelling and simulation, originally based at Imperial College London where he completed his PhD and post-doctoral studies, is now a part-time Assistant Professor within the University of Eindhoven, with focus on battery management systems. He is based in the Netherlands as a senior research scientist within TNO, the Dutch Organization of Applied Research. He is a member of the Powertrains department within TNO, is an active member of EARPA and EGVIA, and is involved in the FABRIC, TRANSFORMERS, CONVENIENT, EMC2, ABattReLife, AMBERULV, ORCA and 3CCar European project amongst others.

Stefan van Sterkenburg received his master's degree and PhD degree from the Eindhoven University of Technology in 1987 and 1991 respectively.

Currently he is researcher in the fields of electrical drive trains and battery technology at the HAN University of Applied Sciences in Arnhem, the Netherlands.

Erik Hoedemaekers, (MSc) obtained his MSc degree in Automotive Technology at the Eindhoven University of Technology, where he specialized in Electromechanics and Power Electronics and graduated on state- and parameter estimation on LFP batteries.
He is currently a research scientist at TNO,the Dutch Organization of Applied Research, in the Powertrains department. His current work includes battery testing, modeling and simulation, as well as state- and parameter estimation, and is involved in different European projects like ABattReLife, AMBER, 3Ccar, amongst others.

Bogdan Rosca obtained his M.Sc. degree in Automotive Technology from the Eindhoven Technical University, in 2011. He is currently a research engineer at TNO, the Dutch Organization of Applied Research, in the Powertrains Department.
His activities include battery modelling and state estimation, powertrain modelling and control and driver behavior characterization. He is currently involved in various European projects:

Dmitri Danilov is post doctoral researcher based at the Technical University of Eindhoven within the Control Systems research group of the Electrical Engineering Department. He has a wide range of battery research related publications and is active in both national and European projects.

Rik Baert has over 30 year of experience in the field of powertrains. He has worked both in academia (PhD from University of Gent, M.Sc. at Manchester University, Assistant Professor at Delft) and industry (DAF Trucks). He has been 12 years Prof. of Internal Combustion Engines at Eindhoven University. He has been project leader of several large powertrain development projects.